

Models of Tokamak Disruptions

H. R. Strauss

HRS Fusion
 West Orange, NJ 07052 USA
 hank@hrsfusion.com

Abstract

Disruptions are a serious issue in tokamaks. In a disruption, the thermal energy is lost by means of an instability which could be a resistive wall tearing mode (RWTM). During precursors to a disruption, the plasma edge region cools, causing the current to contract. Model sequences of contracted current equilibria are given, and their stability is calculated. A linear stability study shows that there is a maximum value of edge $q_a \approx 3$ for RWTMs to occur. This also implies a minimum rational surface radius normalized to plasma radius from RWTMs to be unstable. Nonlinear simulations are performed using a similar model sequence derived from an equilibrium reconstruction. There is a striking difference in the results, depending on whether the wall is ideal or resistive. With an ideal wall, the perturbations saturate at moderate amplitude, causing a minor disruption without a thermal quench. With a resistive wall, there is a major disruption with a thermal quench, if the edge $q_a \leq 3$. There is a sharp transition in nonlinear behavior at $q_a = 3$. This is consistent with the linear model and with experiments. If disruptions are caused by RWTMs, then devices with highly conducting walls, such as the International Tokamak Experimental Reactor (ITER) will experience much milder, tolerable, disruptions than presently predicted.

1 Introduction

Disruptions are a serious issue in tokamaks, the leading magnetic fusion device. Recent work has identified disruptions in JET [1], ITER [2], DIII-D [3], and MST [4, 5] as possibly caused by resistive wall tearing modes (RWTMs) [6, 7, 8]. It was shown in numerical simulations that RWTMs are able to cause a complete thermal quench (TQ). An onset condition for a RWTM is that with an ideal wall, it would be a stable tearing mode (TM). This is consistent with simulations and experimental data.

An object of this paper is to show that experimental conditions for tokamak disruptions are also conditions for RWTM instability. Models are presented which shows that RWTMs can occur when edge cooling causes contraction of the current. The model shows that the rational surface radius r_s must be sufficiently close to the resistive wall, or that the edge q_a be

sufficiently low for RWTMs to occur. The q_a value for RWTM instability is $q_a \lesssim 3$. This is consistent with experiments, which generally run with $q_a > 3$ to avoid disruptions [9]. The onset condition is studied linearly using a sequence of equilibrium models with varying q_a and current contraction, which can be studied semi analytically. The onset condition is also studied nonlinearly, with a more realistic sequence of equilibria with varying q_a . The equilibria are constructed from an MST equilibrium reconstruction [5]. The marginal stability condition for RWTMs is consistent between the two models. The nonlinear simulations illustrate the basic result that RWTMs can cause a thermal quench. There is a striking difference in the simulations with ideal and resistive walls. Nonlinear simulations of the same equilibria with an ideal wall boundary condition only obtain a minor disruption without a TQ. Simulations with a resistive wall obtain a major disruption and TQ, when $q_a \leq 3$. For a resistive wall, there is a sharp transition in the simulations at the RWTM onset condition $q_a = 3$. For $q_a > 3$, the behavior is similar to having an ideal wall.

Disruptions are generally preceded by precursors, which typically involve tearing modes. Numerous causes of precursors in JET have been identified [10], which lead to locked modes. These include neoclassical tearing modes (NTM) [11], and radiative cooling by impurities [12]. Nearly all JET disruptions are preceded by locked modes, but they are not the instability causing the thermal quench. Rather, the locked mode indicates an “unhealthy” plasma which may disrupt [13]. Locked modes are also disruption precursors in DIII-D [14, 15]. The locked modes are tearing modes. They can overlap and cause stochastic thermal transport in the plasma edge region.

During the locked mode phase, edge transport and cooling modify the edge temperature and current. The drop in the edge temperature causes the current to contract, while the total current stays constant. The result has been called [16] a “deficient edge”. It has also been described [15] as “ $T_{e,q2}$ collapse”, a minor disruption of the edge. The edge cooling causes the resistivity in the edge to increase, which increases the growth rate of TMs and RWTMs.

A condition for disruptions is that the $q = 2$ magnetic surface is sufficiently near the plasma edge. This is been documented in DIII-D [14]. It was found that disruptions require the $q = 2$ rational surface radius $r_s > 0.75r_a$, where r_a is the plasma minor radius.

The TQ times found in RWTM simulations are consistent with experiment. In [9] a JET TQ time was given as $0.7ms$, while $1.5ms$ was found in simulations [1]. This is in reasonable agreement with the TQ times calculated [1] from experimental shots listed in the JET ITER - like wall 2011 - 2016 disruption database [13]. The TQ time in a DIII-D simulation [3] agreed with the experimental data. The TQ time in an MST simulation [5] exceeded the experimental pulse time, consistent with the lack of disruptions observed. It was noted [9] that TQ times scaled linearly with machine size, which suggests they are proportional to the Alfvén time. This does not rule out a dependence on resistive wall penetration time τ_{wall} , because all the experiments had similar wall times. An exception is MST [5], which has a wall time of $800ms$.

2 Linear model

Linear MHD stability is studied using a set of model equilibria in a straight periodic cylinder.. The model equilibria are modified FRS [19] profiles. The current density is

$$j(r) = \frac{2}{q_0}(1 + r^{2n})^{-(1+1/n)} \quad (1)$$

It is normalized to B/R , where B is the total magnetic field, $2\pi R$ is the periodicity length, and radius r normalized to the plasma radius. A peaked profile has $n = 1$, rounded, $n = 2$, and flattened, $n = 4$. In this model n is a real number, not restricted to an integer. In order to cut off the current at $r = r_c$, a constant c_r is subtracted, with

$$c_r = (1 + r_c^{2n})^{-(1+1/n)} \quad (2)$$

where r_c is the maximum radius of nonzero current normalized to plasma radius..

$$j(r) = \begin{cases} (2c_0/q_0)[(1 + r^{2n})^{-(1+1/n)} - c_r] & r < r_c \\ 0 & r \geq r_c. \end{cases} \quad (3)$$

The factor $c_0 = 1/(1 - c_r)$ keeps $j(0)$ independent of r_c . This gives a q profile

$$q(r) = \begin{cases} (q_0/c_0)[(1 + r^{2n})^{-1/n} - c_r]^{-1} & r < r_c \\ q(r_c)(r/r_c)^2 & r \geq r_c. \end{cases} \quad (4)$$

Note that the total current is given by

$$I = r_a^2/q_a = r_w^2/q_w, \quad (5)$$

where $q = q_a$ at the plasma edge $r_a = 1$, or by q_w is the value of q at the wall radius normalized to plasma radius r_w .

Sequences of equilibria during a precursor are modeled by keeping $q_0 = 1$, and by fixing q_a to have constant I . During the sequence, r_c is decreased. This causes the profile parameter n to increase, in order to maintain constant q_0, q_a . Current shrinking and broadening occur simultaneously. The change in linear stability during this model sequence is investigated, with both ideal and no wall boundary conditions. Resistive wall tearing modes are tearing stable with an ideal wall, and unstable with no wall.

Rotation is not included. The mode is assumed locked.

The ideal wall tearing stability parameter Δ'_i and the no wall tearing stability parameter Δ'_n are calculated in cylindrical geometry. RWTMs have [1, 3, 5] $\Delta'_i < 0$, and $\Delta'_n > 0$. Linear magnetic perturbations satisfy [6, 18, 19, 20]

$$\frac{1}{r} \frac{d}{dr} r \frac{d\psi}{dr} - \frac{m^2}{r^2} \psi = \frac{m}{r} \frac{dj}{dr} \frac{m/q - n}{[(m/q - n)^2 + m^2 \delta^2]} \psi \quad (6)$$

where the singularity at the rational surface is regularized [18], with $\delta = 10^{-4}$. In case $r_c < r_s$, the right side of (6) vanishes for $r > r_c$, so there is no singularity at r_s and $\psi \propto r^{\pm m}$. Here (m, n) are the poloidal and toroidal mode numbers of a perturbation $\psi(r) \exp(im\theta - in\phi)$, using a large aspect ratio approximation.

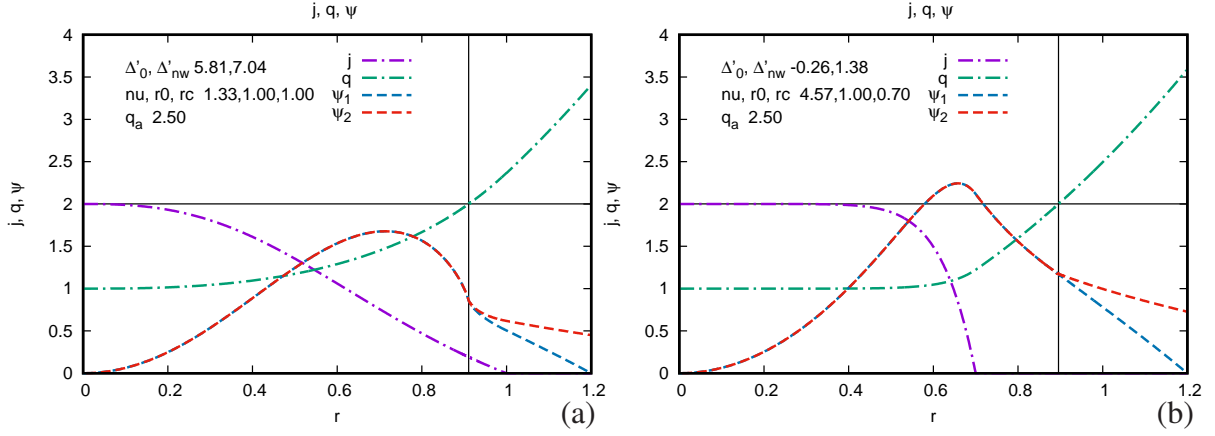


Figure 1: ψ , j , and q , with ψ for ideal (ψ_1) and no wall (ψ_2). (a) tearing mode unstable. The current is nonzero for $r < 1$. (b) RWTM unstable. The current is non zero for $r < r_c = .75$. The current profile is flattened so the total current is almost the same as in (a). In both cases $q_0 = 1$.

Solving with a shooting method, there are two boundary conditions: integrating outward from $r = 0$, and inward from $r = r_w$, the wall radius. The boundary conditions at the origin are $\psi(0) = 0$, $d\psi/dr(0) = 0$, since $\psi \sim r^m$, with $m \geq 2$. At the wall $r = r_w$, an ideal wall boundary condition is $\psi(r_w) = 0$, $d\psi/dr(r_w) = 1$. A resistive wall (or no wall) boundary condition is $\psi(r_w) = 1$, $d\psi/dr(r_w) = -(m/r_w)\psi(r_w)$. The value of Δ' is calculated at r_s at which $q(r_s) = m/n$,

$$\Delta' = \frac{\psi'_+(r_s)}{\psi_+(r_s)} - \frac{\psi'_-(r_s)}{\psi_-(r_s)} \quad (7)$$

where $\psi' = d\psi/dr$, ψ_- is the solution integrated outward from $r = 0$, and ψ_+ is the solution integrated inward from $r = r_w$. For an ideal wall, denote $\Delta' = k_\perp \Delta_i$, while for no wall, $\Delta' = k_\perp \Delta_n$, where $k_\perp = m/r_s$. The RWTM instability condition is $\Delta_i \leq 0$, $\Delta_n \geq 0$.

In the following, $(m, n) = (2, 1)$, which are the dominant mode numbers in typical disruptions.

The effect of the boundary conditions is illustrated in Fig.1(a),(b). The plots show $j(r)$, $q(r)$, and $\psi(r)$ for both ideal wall (ψ_1) and resistive wall (ψ_2). The plasma boundary is $r_a = 1$, and the wall is at $r_w = 1.2$. The values of ψ were normalized so that $\psi_+(r_s) = \psi_-(r_s)$. In each figure the two cases have the same profiles of j and q , as well as the same ψ_- . The profiles of ψ_+ differ. The no wall boundary condition produces a more positive value of Δ' ,

$$\Delta_n - \Delta_i = \Delta_x \geq 0. \quad (8)$$

Fig.1(a),(b) have different $j(r)$ profiles. Both cases have approximately the same total current J and have $q_0 = 1, q_a = 2.5$. In Fig.1(a), j is non zero for $r < 1$. In Fig.1(b), j is non zero for $r < r_c = 0.70$. There is a marked difference in Δ' . The case in Fig.1(a) is unstable to a tearing mode, while the second case in Fig.1(b) is unstable to a RWTM. This supports the conjecture that suppressing the current in the plasma edge region destabilizes the RWTM. The RWTM also requires that r_s be sufficiently close to r_w , so that Δ'_i can become less than zero.

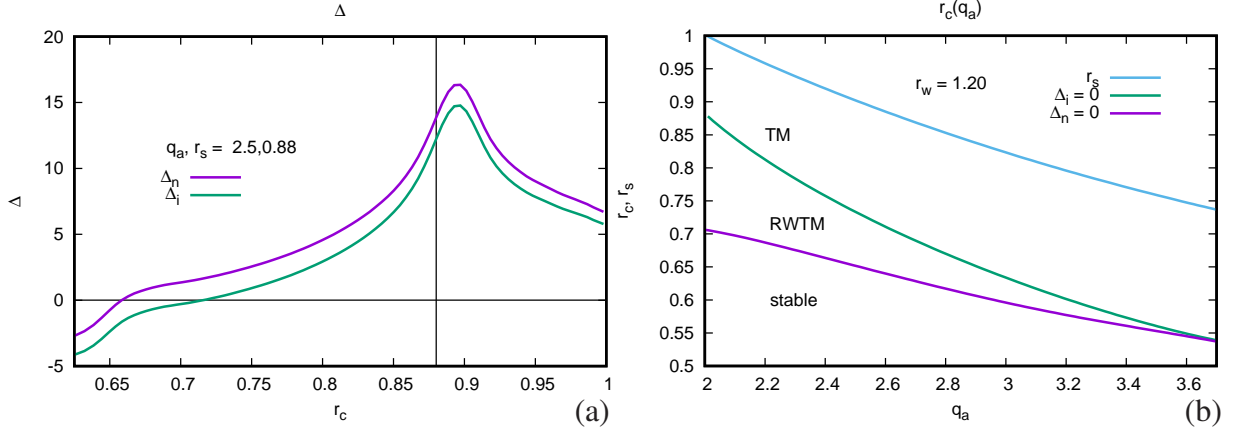


Figure 2: (a) Δ_n, Δ_i , as a function of r_c , for $q_a = 2.5$. $\Delta_i < 0$ for $r_c < 0.8$, and $\Delta_n < 0$ for $r_c < 0.7$. (b) Curves of $\Delta_i(q_a, r_c) = 0$ and $\Delta_n(q_a, r_c) = 0$. The curves join at $q_a \approx 3.5, r_s = .75, r_c = 0.57$.

Fig.2(a) shows how Δ_i, Δ_n vary with the current limiting radius r_c . The rational surface radius $r_s = .88$ and $q_a = 2.5$ are constant. As r_c decreases, at first the TM is destabilized, as Δ_i, Δ_n increase. For more contraction and smaller r_c , the TM is stabilized and the RWTM is destabilized, as the values of Δ_i, Δ_n decrease, with $\Delta_n > \Delta_i$. For $r_c \leq 0.71$, $\Delta_i \leq 0$. This is the onset condition for a RWTM. Further contraction stabilizes the RWTM. For $r_c \leq 0.66$, $\Delta_n \leq 0$. This implies the RWTM is stabilized. There is a range of $0.71 \geq r_c \geq 0.66$ in which the RWTM is unstable.

Fig.2(b) shows how the marginal Δ_i, Δ_n values vary with q_a . The critical values of r_c are found for both $\Delta_i = 0$, and for $\Delta_n = 0$. As in Fig.2(a) there is a gap in r_c between RWTM instability and stability. The curves join at $q_a \approx 3.5, r_s = .75, r_c = 0.57$. For $q_a > 3.5$, the RWTM is stable. The condition for RWTM instability in the model agrees well with condition for disruptions in a DIII-D database [14].

In DIII-D and the linear examples, $r_w/r_a = 1.2$. For larger r_w/r_a , the region of RWTM instability in Fig.2(b) becomes smaller. Fig.3(a) shows the zero curves of Δ_i, Δ_n for $r_w = 1.5$. There is little difference in stability between ideal and resistive wall tearing modes. For larger $r_w/r_a \approx 1.8$, the RWTMs disappear. The modes become no wall tearing modes, whose properties will be studied elsewhere.

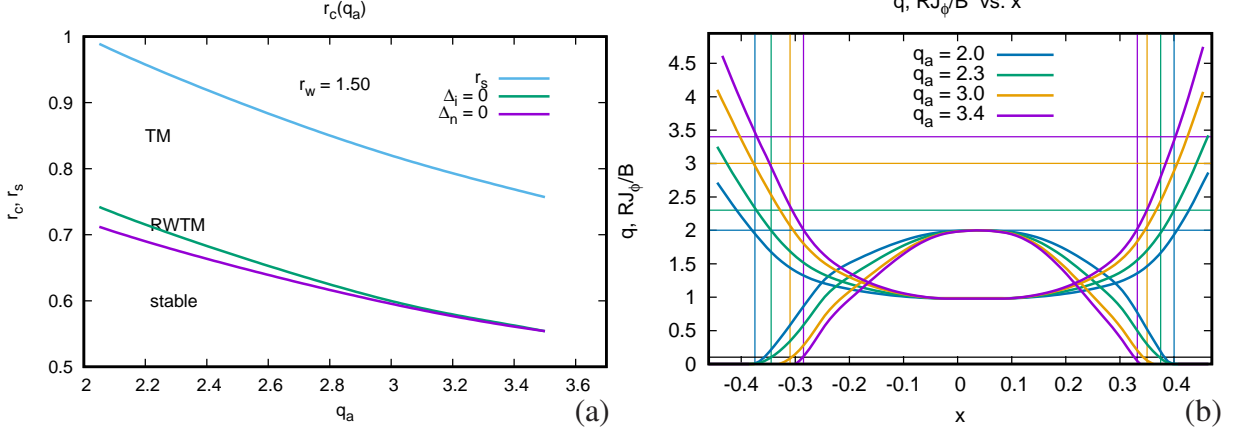


Figure 3: (a) Curves of $\Delta_i(q_a, r_c) = 0$ and $\Delta_n(q_a, r_c) = 0$, with $r_w = 1.5$. There is only a small RWTM unstable region. (b) q and RJ_ϕ/B profiles of a sequence of equilibria derived from MST, with $q_a = 2.0, 2.3, 3.0, 3.4$. At the respective $(2, 1)$ rational surfaces r_s , the current density has less than 5% of its value on axis. The current profile is progressively contracted as q_a increases. The minimum $r_s = 0.8r_a$.

3 Nonlinear thermal quench

Nonlinear simulations were performed with the M3D resistive 3D MHD code [21] including a resistive wall [22], using more realistic equilibria. The equilibria were derived from an MST equilibrium reconstruction [5] with $q_a = 2.0$, which was unstable to a RWTM. The major radius is $R = 1.5m$, and the wall minor radius is $r_w = 0.48m$ in the simulations. The current was constricted away from the wall, with $r_a = 0.4m$, to make the equilibrium more unstable. A set of equilibria was prepared with varying q_a .

The initial current density was $C_1 = R\nabla R^{-1} \cdot \nabla\psi_1$, where ψ_1 is the magnetic flux. In order to vary q_a , a new equilibrium was produced with $C_2 = C_1$ initially. The current C_2 was set to zero outside a particular value of normalized radius $\rho > \rho_a$ which was a flux surface of ψ_1 . In the following, $\rho_a = .83\rho_w$, so $r_w/r_a = 1.2$. The value $C_2(\rho_a)$ was subtracted from C_2 for $\rho \leq \rho_a$. The pressure was modified in the same way. The initial volume averaged $\beta \approx 5 \times 10^{-3}$, so the pressure modification had a negligible effect. A new current density $C = c_1 C_2 + c_2 C_2^2$ with constants c_1, c_2 , was constrained to have $C(0) = 2$ on axis, which gives $q_0 \approx 1$ on axis and volume integral $\int C dV = c_3 \int C_1 dV$, where c_3 is a given constant. This gives two linear equations for c_1, c_2 . The constant c_3 was chosen to give a range of q_a values, where $q = q_a$ is the value at the plasma edge $\rho = \rho_a$.

Initial profiles of q and RJ_ϕ/B as a function of $x = R - R_0$ are shown in Fig.3(b) for $q_a = 2.0, 2.3, 3.0, 3.4$, where R_0 is the magnetic axis. The plasma radius is at $x = \pm 0.4$. Horizontal lines are provided to find q_a , and vertical lines are added to locate r_s , the $q = 2$ rational surface. As q_a increases, r_s decreases. The current density is small at r_s , less than 5%

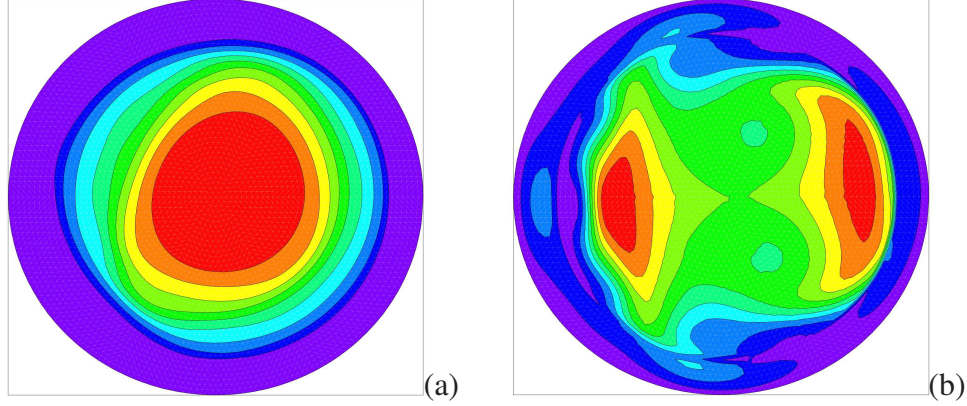


Figure 4: (a) Temperature T contours at $t = 6059\tau_A$, for $q_a = 3.0$, with ideal wall, and saturated $(2, 1)$, $(3, 2)$ modes. (b) temperature T at $t = 6390\tau_A$, $q_a = 3.0$, with resistive wall, $S_{wall} = 10^3$, and a large predominantly $(2, 1)$ island structure.

of its value on axis. This is stabilizing for tearing modes.

The initial profiles in Fig.3(b) are stable according to the local criterion [23],

$$\Delta = -\pi\sigma \cot(\pi\sigma/2), \quad \sigma = J'_\phi/Bk'_\parallel \quad (9)$$

It can be shown that $\sigma \approx RJ_\phi(r_s)/(2B)$, assuming $J'_\phi \approx -J_\phi(r_s)/r_s$. From Fig.3(a), $\sigma \approx 0.125$. In order to have $\Delta > 0$, it is required that $\sigma > 1$. This does not include no wall destabilization.

Nonlinear runs were carried out with the parameters of MST simulations [5]: Lundquist number $S = 10^5$, and parallel thermal conductivity $\chi_\parallel = 10Rv_A$. The wall time was taken much shorter than in MST, $S_{wall} = 10^3$, in order to speed up the simulations. Here $S_{wall} = \tau_{wall}/\tau_A$, where τ_{wall} is the resistive wall magnetic penetration time and $\tau_A = R/v_A$ is the Alfvén time, with Alfvén velocity v_A and major radius R . In MST, $\tau_A = 1.15 \times 10^{-6}s$.

Examples of temperature T contours in nonlinear simulations are shown in Fig.4, with $q_a = 3.0$. Fig.4(a) shows T at time $t = 6059\tau_A$, with an ideal wall. The perturbations involve $(2, 1)$ and $(3, 2)$ modes. Fig.4(b) shows T contours at time $t = 6390\tau_A$ with a resistive wall, $S_{wall} = 10^3$. Modes $(2, 1)$ and $(3, 2)$ have larger amplitude than in the ideal wall case Fig.4(a). There is a large predominantly $(2, 1)$ island structure. Evidently the initial state was not quite in equilibrium. It relaxed to an unstable state. It is clear that the resistive wall has a great effect on the mode evolution.

Fig.5(a) shows time histories of total pressure P with an ideal wall, for cases with $q_a = 3.4, 3.0, 2.3$, and 2.0 . There are only minor disruptions, with a moderate decrease in P .

With a resistive wall, the results are quite different. Fig.5(b) shows time histories of total pressure P and $10^3 b_n$ for cases with $q_a = 3.4, 3.0, 2.3$, and 2.0 . Here b_n is the toroidally

varying normal magnetic field perturbation at the wall, normalized to the toroidal magnetic field. With an ideal wall $b_n = 0$. For $q_a = 3.0, 2.3, 2.0$ there is a major disruption. This will be defined as a loss of more than 80% of the total pressure P . For $q_a = 3.4$ there is a minor disruption.

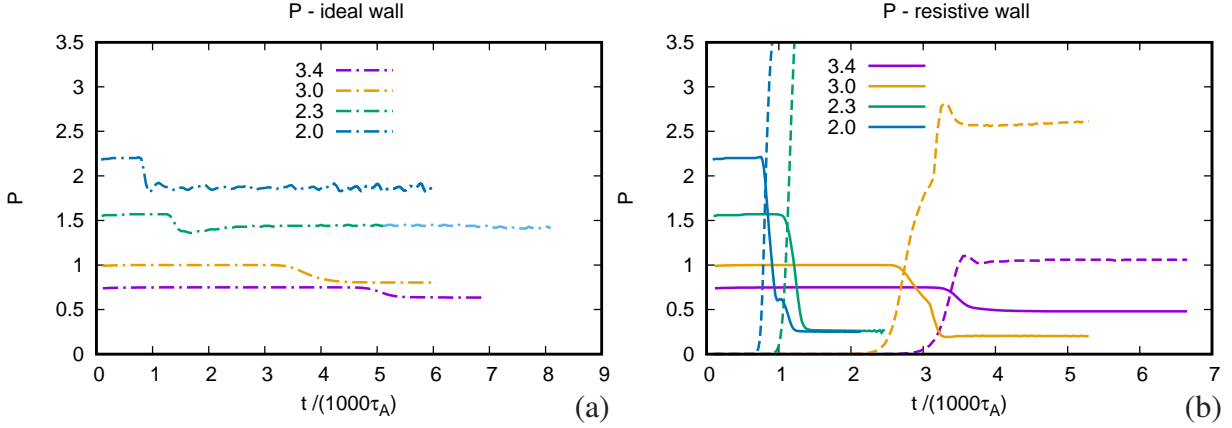


Figure 5: (a) time histories in units of $1000\tau_A$ of total pressure P in nonlinear simulations of MST with profiles of Fig.3(a), with ideal wall. There are only minor disruptions. (b) P and b_n as a function of $t/(1000\tau_A)$ for the same initial profiles, for resistive wall with $S_{wall} = 10^3$.

The TQ time τ_{TQ} varies with q_a . For $q_a \geq 3.1$ the mode is a TM which does not cause a TQ. Fig.6(a) shows τ_{TQ} and $1/\gamma$ obtained from Fig.5(b), as functions of q_a . The value of $\tau_{TQ} = (t_2 - t_9)/(.9 - P_2/P_{max})$ where t_2 is the time in τ_A units at which $P = P_2 = .2P_{max}$, and similarly for t_9 . If there is only a minor disruption for which there is no value of t_2 , then t_2 is replaced by t_{last} , and $P_2 = P_{last}$, at the longest time for that particular simulation. This is an under estimate, but it shows that τ_{TQ} is much smaller in the RWTM regime $q_a \leq 3$. At $q_a = 3$, using the MST Alfvén time, $\tau_{TQ} = 0.6ms$. This is two orders of magnitude faster than τ_{TQ} calculated in the MST experiment [5]. At higher q_a there should be no RWTMs. The growth rate γ of b_n is calculated. The relation $\tau_{TQ} = 1/\gamma$ which is well satisfied for $2 \leq q_a \leq 3.0$, is characteristic of RWTMs [1]. The stability boundary is consistent with the linear model Fig.3(b), for which the onset condition is $q_a \approx 3.5$. This is reasonable, considering that the current profiles are different, and the RWTM regime is small for $q_a > 3$.

Fig.6(b) shows the maximum value of $10^2 b_n$ and $\xi = c_0 b_n^{1/2} r_s$, where ξ is an island width [24], with $c_0 = 4(2R/r_s)^{1/2}(r_w/r_s)^{3/2}$. The magnetic perturbation at the rational surface is $(r_w/r_s)^3 b_n$. Also shown are two measures of the change in total pressure: $\Delta_1 P = 1 - P_{min}/P_{max}$, and $\Delta_2 P = (P_{max}/P_{min} - 1)/7$, as a function of q_a . There is a marked jump in these quantities at $q_a = 3$. The correlation of ξ , $\Delta_1 P$, $\Delta_2 P$ for $2 \leq q_a \leq 3$ suggests the transport is advective, with $\delta P \approx -\xi P'$. The approximation $\Delta P_2 = \xi/r_s$ has the appropriate amplitude but a better fit is made using $\Delta P_2 = \xi/r_s$.

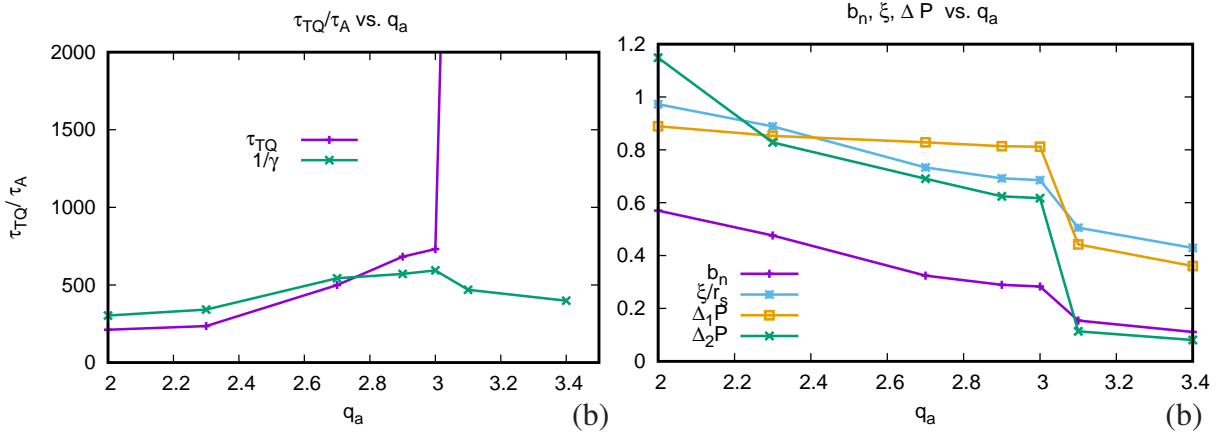


Figure 6: (a) τ_{TQ}/τ_A and $1/\gamma$ from time histories, as a function of q_a . There is an abrupt lengthening of the TQ time for $q_a > 3$. The TQ time is approximately equal to the growth time $1/\gamma$, which is typical of RWTMs. Additional time histories with $q_a = 2.7, 2.9, 3.1$ are included. (b) $10^2 b_n$, $\Delta_1 P = (1 - P_{min}/P_{max})$, $\Delta_2 P = (P_{max}/P_{min} - 1)/7$, and $\xi = c_0 b_n^{1/2} r_s$ as a function of q_a . The quantity ξ is an island width, where $c_0 = 12.9$. These quantities are correlated, with a marked jump at $q_a = 3$.

4 Conclusion

Disruption precursors have many causes, leading to locked modes in JET and DIII-D. During precursors, the edge temperature is reduced, causing the current to contract. Disruption onset requires the $q = 2$ rational surface to be sufficiently close to the plasma edge. This is consistent with RWTM destabilization. Two sets of model equilibria are given which includes current contraction, while maintaining constant total current and $q = 1$ on axis. The first set is analyzed with linear MHD equations, and solved with ideal wall and no wall boundary conditions. No wall boundary conditions always make the tearing mode more unstable than with an ideal wall. If a tearing mode is stable with an ideal wall and unstable with no wall, it is a resistive wall tearing mode. The model is consistent with experimental disruption thresholds. For a sufficiently large $(2, 1)$ rational surface radius r_s , shrinking the current radius r_c destabilizes the RWTM. Further shrinking of r_c stabilizes the RWTM, which exists in a range of r_c values. The model shows that there a maximum value of q_a for which instability is possible.

The second, more realistic set of equilibria was used to initialize nonlinear simulations. The simulations show a striking difference between ideal and resistive wall. A sequence of initial states with different q_a was prepared from an MST equilibrium reconstruction. These states were contracted inward from the wall, and had very small values of toroidal current at the $(2, 1)$ rational surface. For an ideal wall, minor disruptions occurred. For a resistive wall, minor disruptions occurred if $q_a > 3$. For a resistive wall and edge $q_a \leq 3$, major disruptions occurred. There was a sharp transition in disruptive behavior at the critical value $q_a = 3$. This

indicates that the thermal quench was produced by RWTMs, and also shows that their onset condition agrees with well known experimental experience [9].

This work provides additional evidence from theory, simulation, and experimental data that disruptions can be caused by resistive wall tearing modes. MST and ITER have highly conducting walls, so RWTM disruptions are slow. RWTMs cause “soft disruptions,” which can be passively slowed. The RWTM disruptions are low β . High β disruptions are resistive wall modes (RWM) [25], which can also be passively slowed. “Hard disruptions” can occur with an ideal wall, and are caused by making highly unstable equilibria, using MGI [26], SPI [27] or highly unstable initial conditions in simulations [28].

If hard disruptions are avoided, then devices with highly conducting walls such as ITER [2] could experience much milder, tolerable disruptions than presently predicted [9].

Acknowledgement This work was supported by USDOE grant DE-SC0020127.

References

- [1] H. Strauss and JET Contributors, Effect of Resistive Wall on Thermal Quench in JET Disruptions, *Phys. Plasmas* **28**, 032501 (2021)
- [2] H. Strauss, Thermal quench in ITER disruptions, *Phys. Plasmas* **28** 072507 (2021)
- [3] H. Strauss, B. C. Lyons, M. Knolker, Locked mode disruptions in DIII-D and application to ITER, *Phys. Plasmas* **29** 112508 (2022).
- [4] N. C. Hurst, B. E. Chapman, A. F. Almagri, B. S. Cornille, S. Z. Kubala, K. J. McCollam, J. S. Sarff, C. R. Sovinec, J. K. Anderson, D. J. Den Hartog, C. B. Forest, M. D. Pandya, and W. S. Solsrud, Self-organized magnetic equilibria in tokamak plasmas with very low edge safety factor, *Phys. Plasmas* **29** 080704 2022.
- [5] H. R. Strauss, B. E. Chapman, N. C. Hurst, MST Resistive Wall Tearing Mode Simulations, *Plasma Phys. Control. Fusion* **65** 084002 (2023); <https://doi.org/10.1088/1361-6587/acdff8>
- [6] John A. Finn, Stabilization of ideal plasma resistive wall modes in cylindrical geometry: the effect of resistive layers, *Phys. Plasmas* **2**, 3782 (1995)
- [7] C.G. Gimblett, On free boundary instabilities induced by a resistive wall, *Nucl. Fusion* **26** 617 (1986)
- [8] A. Bondeson and M. Persson, Stabilization by resistive walls and q-limit disruptions in tokamaks, *Nucl. Fusion* **28** 1887 (1988)
- [9] ITER Physics Expert Group on Disruptions, Plasma Control, and MHD: S. Mirnov, J. Wesley, N. Fujisawa, Yu. Gribov, O. Gruber, T. Hender, N. Ivanov, S. Jardin, J. Lister, F. W. Perkins, M. Rosenbluth, N. Sauthoff, T. Taylor, S. Tokuda, K. Yamazaki, R. Yoshino,

- A. Bondeson, J. Conner, E. Fredrickson, D. Gates, R. Granetz, R. La Haye, J. Neuhauser, F. Porcelli, D.E. Post, N.A. Uckan, M. Azumi, D.J. Campbell, M. Wakatani, W.M. Nevins, M. Shimada, J. Van Dam, ITER Physics Basis Chapter 3: MHD stability, operational limits and disruptions, *Nuclear Fusion*, **39**, 2251 (1999).
- [10] P.C. de Vries, M.F. Johnson, B. Alper, P. Buratti, T.C. Hender, H.R. Koslowski, V. Riccardo and JET-EFDA Contributors, Survey of disruption causes at JET, *Nucl. Fusion* **51** 053018 (2011).‘
- [11] R.J. La Haye, C. Chrystal , E.J. Strait , J.D. Callen, C.C. Hegna, E.C. Howell , M. Okabayashi and R.S. Wilcox, Disruptive neoclassical tearing mode seeding in DIII-D with implications for ITER, *Nucl. Fusion* **62** 056017 (2022).
- [12] G. Pucella, P. Buratti, E. Giovannozzi, E. Alessi, F. Auriemma, D. Brunetti, D. R. Ferreira, M. Baruzzo, D. Frigione, L. Garzotti, E. Joffrin, E. Lerche, P. J. Lomas, S. Nowak, L. Piron, F. Rimini, C. Sozzi, D. Van Eester, and JET Contributors, Tearing modes in plasma termination on JET: the role of temperature hollowing and edge cooling, *Nucl. Fusion* **61** 046020 (2021)
- [13] S.N. Gerasimov, P. Abreu, G Artaserse, M. Baruzzo, P. Buratti, I.S. Carvalho, I.H. Coffey, E. de la Luna, T.C. Hender, R.B. Henriques, R. Felton, S. Jachmich, U. Kruezi, P.J. Lomas, P. McCullen, M. Maslov, E. Matveeva, S. Moradi, L. Piron, F.G. Rimini, W. Schippers, G. Szepesi, M. Tsalas, L.E. Zakharov and JET Contributors, Overview of disruptions with JET-ILW, *Nucl. Fusion* **60** 066028 (2020).
- [14] R. Sweeney, W. Choi, R. J. La Haye, S. Mao, K. E. J. Olofsson, F. A. Volpe, and the DIII-D Team, Statistical analysis of $m/n = 2/1$ locked and quasi - stationary modes with rotating precursors in DIII-D, *Nucl. Fusion* **57** 0160192 (2017)
- [15] R. Sweeney, W. Choi, M. Austin, M. Brookman, V. Izzo, M. Knolker, R.J. La Haye, A. Leonard , E. Strait, F.A. Volpe and The DIII-D Team, Relationship between locked modes and thermal quenches in DIII-D, *Nucl. Fusion* **58** 056022 (2018).
- [16] F.C. Schuller, Disruptions in tokamaks, *Plasma Phys. Controlled Fusion* **37**, A135 (1995).
- [17] J.A. Wesson, R.D. Gill, M. Hugon, F.C. Schuller, J.A. Snipes, D.J. Ward, D.V. Bartlett, D.J. Campbell, P.A. Duperrex, A.W. Edwards, R.S. Granetz, N.A.O. Gottardi, T.C. Hender, E. Lazzaro, P.J. Lomas, N. Lopes Cardozo, K. F. Mast, M.F.F. Nave, N.A. Salmon, P. Smeulders, P.R. Thomas, B.J.D. Tubbing, M.F. Turner, A. Weller, Disruptions in JET, *Nucl. Fusion* **29** 641 (1989).
- [18] C. Z. Cheng, P. Furth and A. H. Boozer, MHD stable regime of the Tokamak, *Plasma Phys. Control. Fusion* **29** 351 (1987).
- [19] H. P. Furth, P. H. Rutherford, and H. Selberg, Tearing mode in the cylindrical tokamak, *Physics of Fluids* **16** 1054 (1973)

- [20] H. P. Furth, J. Killeen, and M. N. Rosenbluth, Finite-Resistivity Instabilities of a Sheet Pinch, *Phys. Fl.* **6**, 459 (1963).
- [21] W. Park, E. Belova, G. Y. Fu, X. Tang, H. R. Strauss, L. E. Sugiyama, Plasma Simulation Studies using Multilevel Physics Models, *Phys. Plasmas* **6** 1796 (1999).
- [22] Alexander Pletzer and H. R. Strauss, An efficient method for solving elliptic boundary element problems with application to the tokamak vacuum problem, *Comput. Phys. Commun.* **182**, 2077 (2011).
- [23] H. R. Strauss, Resistive ballooning modes, *Phys. Fluids* **24**, 2004 (1981)
- [24] P. H. Rutherford, Nonlinear growth of the tearing mode, *Physics of Fluids* **16**, 1903–1908 (1973).
- [25] A.M. Garofalo, G.L. Jackson, R.J. La Haye, M. Okabayashi³, H. Reimerdes, E.J. Strait, J.R. Ferron, R.J. Groebner, Y. In, M.J. Lanctot, G. Matsunaga, G.A. Navratil, W.M. Solomon, H. Takahashi³, M. Takechi, A.D. Turnbull and the DIII-D Team, Stability and control of resistive wall modes in high beta, low rotation DIII-D plasmas, *Nucl. Fusion* **47** 1121–1130 (2007).
- [26] V. A. Izzo, A numerical investigation of the effects of impurity penetration depth on disruption mitigation by massive high-pressure gas jet, *Nucl. Fusion* **46** 541 (2006).
- [27] D. Hu, E. Nardon, M. Hoelzl, F. Wieschollek, M. Lehnen, G. T. A. Huijsmans, D. C. van Vugt, S-H. Kim, JET Contributors and JOEKE Team, Radiation asymmetry and MHD destabilization during the thermal quench after impurity shattered pellet injection, *Nucl. Fusion* **61** 026015 (2021).
- [28] B. V. Waddell, B. Carreras, H. R. Hicks, J. A. Holmes and D. K. Lee, Mechanism for major disruptions in tokamaks, *Phys. Rev. Lett.* **41** 1386 (1978).